Experimental Study on Oscillatory Combustion in Solid-Propellant Motors

T. Koreki,* I. Aoki,* K. Shirota,† and Y. Toda‡
Nissan Motor Co., Ltd., Tokyo, Japan
and
K. Kuratani§
Univeristy of Tokyo, Tokyo, Japan

The relationship between the longitudinal mode oscillatory combustion phenomena in solid-propellant motors and the motor configuration is experimentally examined using small test motors with various grain configurations. The test results show that the establishment of longitudinal oscillation closely relates to a change of the port area along the motor axis, the internal gas flow conditions, and the motor slenderness. The effects of these parameters on the motor design criterion are qualitatively discussed in relation to the propellant response function and the agglomerative burning of aluminum particles. The test results of an effective mechanical suppression device applied to an actual sounding rocket motor are also presented.

Introduction

THE University of Tokyo has developed a single-stage sounding rocket S-310 equipped with a motor having a dual-thrust solid-propellant grain, as shown in Fig. 1a. This propellant consists of 19% polybutadiene, 64% ammonium perchlorate, 17% aluminum, and 2% additives. In the first static firing test of the motor, the authors observed a longitudinal pressure oscillation with an amplitude of about 2 kg/cm^2 and a frequency of 110 Hz from 4.5 sec after ignition. The pressure- and thrust-time histories are shown in Fig. 1b.

The shape of the igniter is shown in Fig. 1c. The igniter case is made of fiber reinforced plastics (FRP) and the main charge consists of pellets which contain boron and potassium nitrate. The pressure-time history in the igniter case and the initial combustion pressure in the rocket motor are shown as a dotted line and a solid line, respectively, in Fig. 1d.

In the first launching, corresponding to the longitudinal oscillation, an axial acceleration with an amplitude of 15 g was observed as predicted from the static firing test. This unacceptable value of acceleration forced the authors to investigate the mechanism and conditions which initiated the pressure oscillation.

Some investigators have presented stable-unstable criteria which were based on the sum of the growth and decay rates of the pressure oscillation.[1,2,3] The experimental verification of these criteria, however, was not necessarily sufficient. Few experimental studies on the ballistic characteristics influencing the longitudinal pressure oscillation have been reported. Among the number of ballistic and acoustic parameters which govern combustion instability, the grain configuration and suppression devices such as the baffle were examined extensively.

Presented as Paper 75-1333 at the AIAA/SAE 11th Propulsion Conference, Anaheim, Calif., Sept. 29-Oct. 1, 1975; submitted Nov. 7, 1975; revision received March 30, 1976. The authors wish to express their sincere thanks to S. Kumagai, Professor Emeritus, University of Tokyo, for his kind guidance in this investigation.

Index categories: Combustion Stability, Ignition, and Detonation; Fuels and Propellant, Properties of; Solid and Hybrid Rocket Engines.

*Engineer, Aeronautical /Space Division.
† Manager, Aeronuatical / Space Division.
‡Director. Member AIAA.
§Professor, Institute of Space and Aeronautical Science.

Experimental Design

Small test motors (shown in Fig. 2) were used in order to study the relation between the grain configurayion and pressure oscillation. In this figure, D_f, D_a, L, and D_t denote the forward-end port diameter, aft-end port diameter, grain or chamber length, and nozzle-throat diameter, respectively. Forty test motors with various grain configurations were used in the experiments. They are shown in Tables 1-7. The propellant composition was 23% polyurethane, 67% ammonium perchlorate, and 10% aluminum. Its burning rate and pressure exponent were 6.5 mm/sec at 50 kg/cm^2 and 0.1, respectively. The authors adopted this formulation, which was more unstable than that of the sounding rocket S-310, which did not show any pressure oscillation in the tests using the small motors.

The igniter was made of granular charges enclosed in a thin polyethylene sheet, and was set in the forward end port of the propellant grain. The main contents of the charge were boron and potassium nitrate. The pressure peaks at the ignition were too small, however, to excite the oscillation in the test motors.

The pressure measurements were conducted using a strain-gage type transducer. On the other hand, for the oscillation measurements, a piezo type transducer and a high-pass filter with a cut-off frequency of 200 Hz, were used. The maximum frequency response of this instrument system was about 10,000 Hz.

Results and Discussion

Several examples of pressure-time histories and pressure oscillations are shown in Figs. 3a-d. It was found that the observed oscillations are of two types of appearance. The first type has only a small amplitude without any change in predicted pressure-time histories, as shown in Fig. 3a. In this case, once the oscillation occurs, it continues until the grain burns out, and its amplitude is found to assume a constant value of 2 kg/cm^2 reproducibility of experiments being assumed. This may be the so-called pressure-coupled instability.

The second type is defined as the oscillation with a large amplitude, which takes place succeeding the first type of oscillation, and is accompanied by a sudden pressure increase, as shown in Fig. 3b. Its occurrence is found not to be reproducible and is considered to be caused by an accidental ejection of the aft-end restrictor fragments, due to the fact that it is never observed in the propellant grains with no aft-

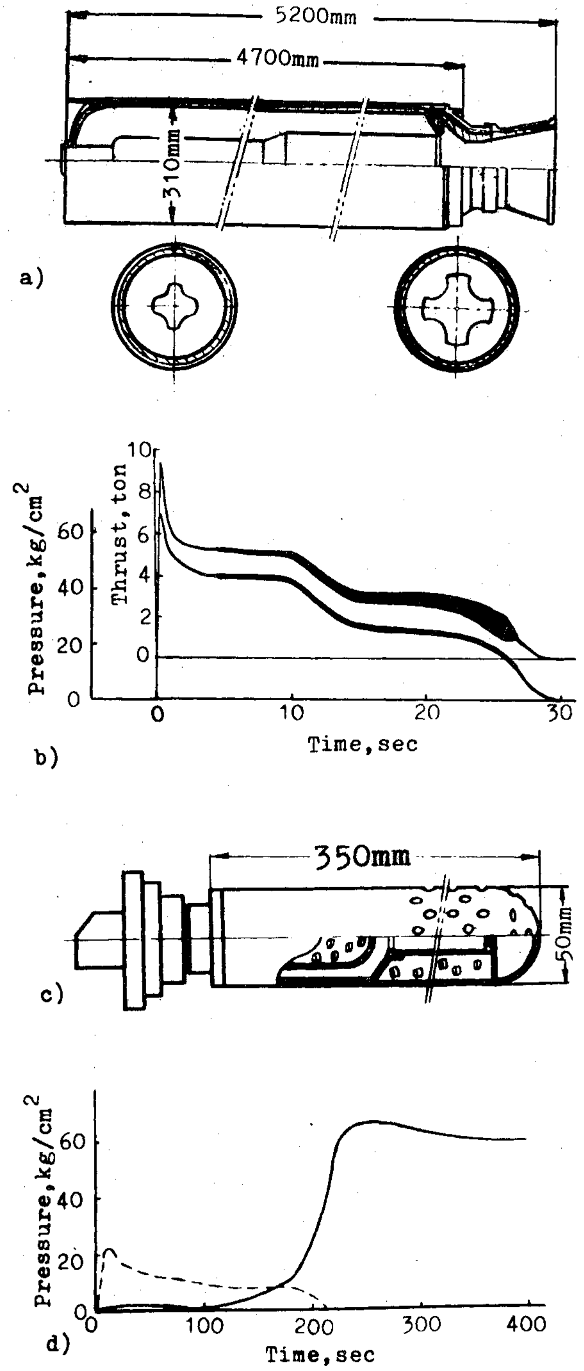

Fig. 1 a) Motor of sounding rocket S-310. b) Pressure and thrust-time histories. c) Structure of igniter. d) Relation between pressure in an igniter and in a motor.

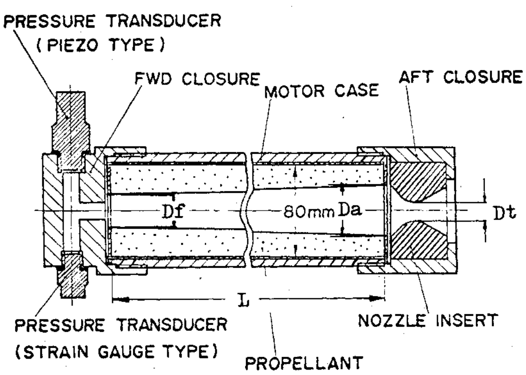

Fig. 2 Small test motor.

Table 1 Effect of step and edge

No.	GRAIN CONFIGURATION	D_f (mm)	D_a (mm)	D_t (mm)	L (mm)	T_g (sec)	P_g (kg/cm^2)
2	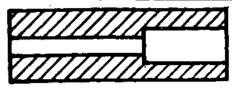	20	40	30	1300	1.25 1.30 1.30	55 52 52
4	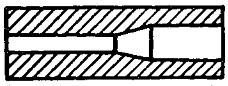	20	40	30	1300	1.25	50
5	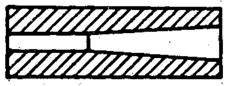	20	40	32	1300	2.05	48
6	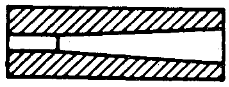	20	40	32	1300	1.75	50
7	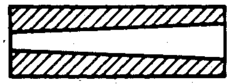	20	40	30	1300	(NO)	-
11	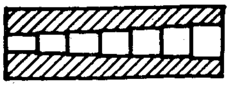	20	40	30	1300	1.35 1.10	52 49
8	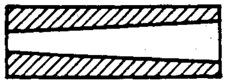	25	45	30	1300	(NO)	-
24	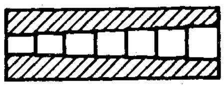	25	45	30	1300	0.75 0.90	54 54

end restrictors in the other auxiliary tests. This may be due to the so-called velocity-coupled instability factor. The present investigation deals exclusively with the first type of oscillation.

In Tables 1-7, T_g denotes the time required for the initiation of the first type oscillation after ignition. In the columns of T_g "NO" underates that oscillation did not occur at all and "(NO)" indicated that oscillation did not occur except at the tail of the pressure-time history, as shown in Fig. 3c.

An oscillation similar to the second type was observed only occasionally at the tail of the pressure-time history, as shown in Fig. 3d. The particular oscillations shown in Figs. 3c and d are assumed to occur from the ejection of the insulator char.

P_g in the tables denotes the combustion pressure at the time T_g. Two or three data points of T_g and P_g in an identical motor configuration number were obtained from two or three experiments which were made to check their reproducibility.

Relation between Oscillation and Grain Configuration

Effects of Step and Edge on the Burning Surface

In Table 1, the initial diameters of the forward- and aft-end ports are unchanged except for Nos. 8, 24, and 9. Numbers 2-6 show an oscillation of about 2 kg/cm^2 amplitude. On the other hand, in No.7 (which has no edge on its burning surface) the oscillation was not observed. In comparing the structures of No. 7 with No. 11 and No. 8 with No. 24, Nos. 7 and 8 have port configurations widening smoothly, while Nos. 11 and 24 have those widening stepwise. The oscillation occurs only in Nos. 11 and 24. These results suggest that steps or edges on the burning surface, from which small eddy currents may propagate, excite the oscillations. These eddy currents

Table 2 Effect of port divergence

No.	GRAIN CONFIGURATION	D_f (mm)	D_a (mm)	D_t (mm)	L (mm)	T_g (sec)	P_g (kg/cm^2)
11	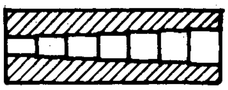	20	40	30	1300	1.35 1.10	52 49
19	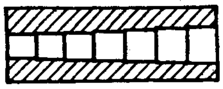	30	40	30	1300	(NO)	–
20	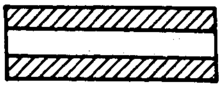	30	30	30	1300	(NO)	–
21		40	40	30	1300	(NO)	–
22	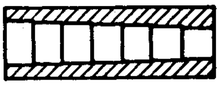	50	40	30	1300	NO	–
23	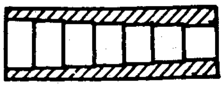	60	40	30	1300	NO	–
35	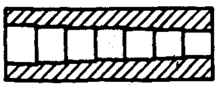	50	30	30	1300	NO	–
25	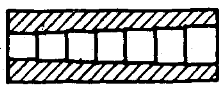	30	50	30	1300	0.5	57
9	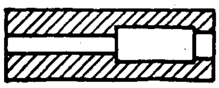	20	30	30	1300	1.30	48

Table 3 Effect of nozzle throat diameter

No.	GRAIN CONFIGURATION	D_f (mm)	D_a (mm)	D_t (mm)	L (mm)	T_g (sec)	P_g (kg/cm^2)
1				26.5	1300	0.90 0.95	64 65
2	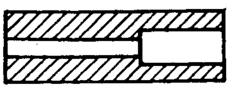	20	40	30	1300	1.25 1.30 1.30	55 52 52
3				33	1300	1.75 1.70	48 45
10				26.5	1300	0.65	65
11	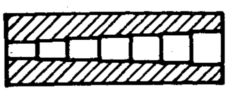	20	40	30	1300	1.35 1.10	52 49
12				33	1300	NO	–

are generally considered to act as both an exciting and a suppressing force, but the former seems stronger than the latter in this experiment.

Effect of Port Divergence

From the comparison of No. 11 with No. 19 in Table 2, it was found that, even with many edges, a gradually widening port configuration was likely to be more effective in suppressing the oscillation. The results obtained in these experiments show that the oscillation occurs in port configurations that widen stepwise above a certain angle. Straight and convergent port configurations such as Nos. 20-23 and 35 suppress the oscillation. Configuration No. 25, whose forward- and aft-end ports are reversed as compared with No. 35, supresses the oscillation. Therefore, in the convergent port, the oscillation was suppressed. However, No. 19, whose port area decreased at the aft-end and increased stepwise near the middle point of the grain, exhibited oscillation.

Compared to the straight, convergent port and the port widening below a certain angle, it is relatively difficult for the eddy current to be generated with the port sharply widening stepwise. Therefore, these results suggest that this port divergence effect actually amplifies the effect of the step and edge on the burning surface.

Table 4 Effect of grain length

No.	GRAIN CONFIGURATION	D_f (mm)	D_a (mm)	D_t (mm)	L (mm)	T_g (sec)	P_g (kg/cm^2)
11				30	1300	1.35 1.10	52 49
13				30	1200	1.60	46
14				30	1100	(NO)	–
15	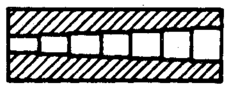	20	40	30	1000	(NO)	–
16				30	600	NO	–
17				26.5	1000	(NO)	–
18				20.4	600	(NO)	–

Table 5 Effect of induction time in rocket motors

No.	GRAIN CONFIGURATION	D_f (mm)	D_a (mm)	D_t (mm)	L (mm)	T_g (sec)	P_g (kg/cm^2)
11	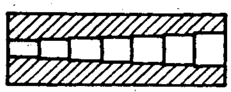	20	40	30	1300	1.35 1.10	52 49
24	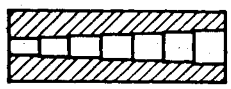	25	45	30	1300	0.75 0.90	54 54
25	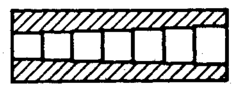	30	50	30	1300	0.50	57
26	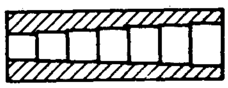	35	55	30	1300	(NO)	–
27	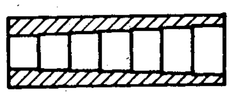	40	60	30	1300	(NO)	–

Effect of Nozzle Throat Diameter

The rocket motors of Nos. 1-3 in Table 3 have the same grain configuration with different throat diameters. It was found that the initiation time T_g increases with the nozzle throat diameter. T_g will closely relate to the particular shape of the port when the oscillation begins. The aft-end port

Table 6 Comparison of experimental and predicted initiation times

No.	Experimental T_g (sec)		Predicted T_g (sec)
5	2.05		1.5
6	1.75		1.55
10	0.65		0.2 → NO
11	1.35	1.10	1.0
12	NO		2.0
13	1.60		1.6
14	NO		2.6
15	NO		NO
16	NO		NO
17	NO		NO
18	NO		NO
19	NO		1.45 → NO
20	NO		2.0 → NO
21	NO		1.5 → NO
22	NO		2.0 → NO
23	NO		NO
24	0.75	0.90	0.75
25	0.50		0.55
26	NO		0.35 → NO
27	NO		0.1 → NO

Table 7 Effect of suppression devices

No.	GRAIN CONFIGURATION	D_b (mm)	D_t (mm)	T_g (sec)	P_g (kg/cm²)
28	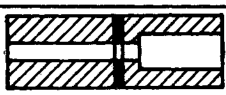	20	30	NO	–
29	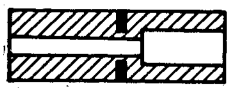	30	30	NO	–
30	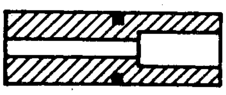	45	30	1.30	51
31	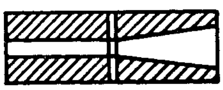	20	30	NO	–
32	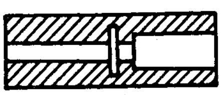	60	30	1.30	52
33	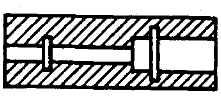	FWD:40 AFT:50	30	1.50	55
34	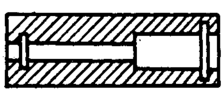	FWD:60 AFT:60	30	1.90	59

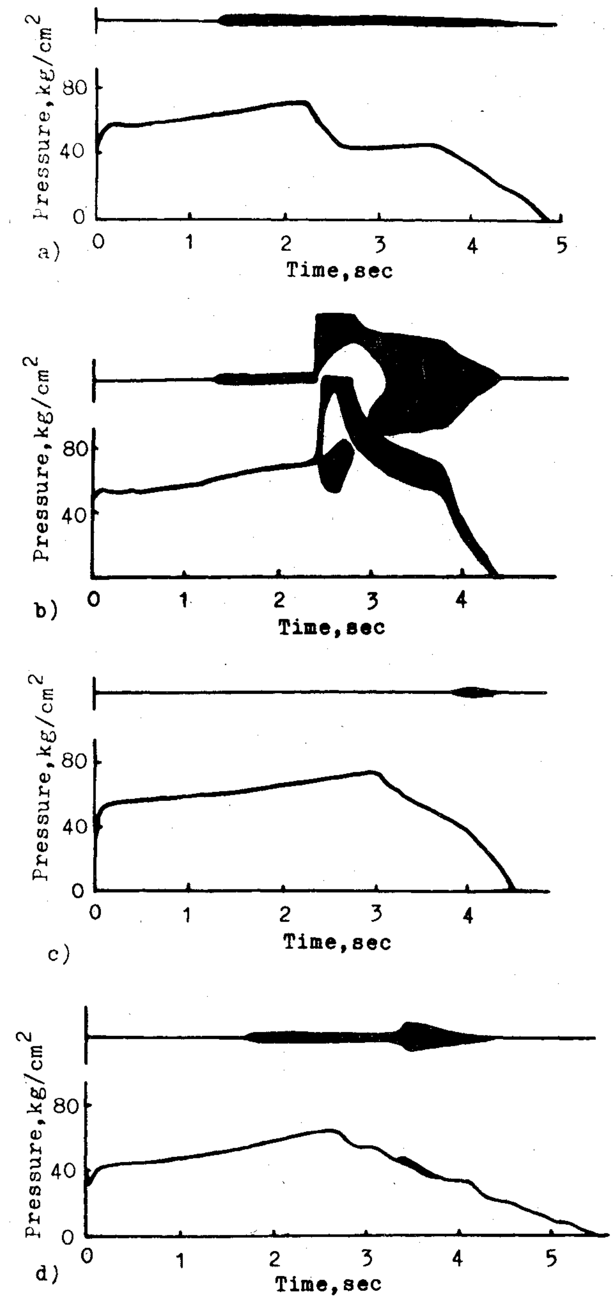

Fig. 3 Typical pressure-time histories and pressure oscillations a), b) Configuration No. 2; c) Configuration No. 20; d) Configuration No. 13.

diameters at the initiation time D_{ag}, which can be calculated from the ballistic parameters, and the ratios J of nozzle throat area to aft-end port area are shown as follows:

No.1	$D_{ag} \simeq 58$ mm	$J = 0.21$
No. 2	$D_{ag} \simeq 64$ mm	$J = 0.22$
No.3	$D_{ag} \simeq 71$ mm	$J = 0.22$

Note that T_g and D_{ag} increase with the throat diameter and J is almost unchanged. The experiments of Nos. 10 and 11 present a similar tendency, as follows:

No. 10	$D_{ag} \simeq 51$ mm	$J = 0.26$
No. 11	$D_{ag} \simeq 61$ mm	$J = 0.24$

These results suggest that oscillation begins at a specified value of J and they permit the possibility of the existence of a critical gas velocity at the aft-end port. The motor of No. 12 does not show any oscillation, because steps in the port probably were too small to excite the oscillation at the end of the burning time.

Effect of Gain Length

The rocket motors of Nos. 11, and 13-16 in Table 4 have gains and chambers of various lengths and nozzles of identical throat diameter. In Nos. 11, 17, and 18, K_n and therefore the chamber pressure are equal to each other. Among these motors, Nos. 14-18 did not show oscillations. These motors have gains less than 1,100 mm, that is, the L/D is less than 14. Comparing No. 11 with No. 13, it was found that T_g increased as L decreased.

The mean pressure of No. 13, which showed oscillations, was 46 kg/cm^2 while the mean pressures of Nos. 14 and 16, which did not show oscillations, were below 42 kg/cm^2. These results would suggest an incipient pressure level below which pressure oscillations did not start. These results, however, are not conclusive. More detailed discussion about the physical meaning of the effects of grain length and nozzle throat diameter on T_g will be conducted at the end of this section.

Time Required for Initiation of Oscillation

From the previous discussion, T_g is considered to depend upon both J and L/D under the existence of small steps and edges. However, T_g may depend not only on such parameters but also on the induction time required for exciting the oscillation. The authors tried to estimate the induction time in Nos. 11 and 24-27, where the web thickness becomes thinner by 2.5 mm from top to bottom (shown in Table 5). In Nos. 11, 24, and 25, oscillation was established at about 1.3 sec, 0.8 sec, and 0.5 sec, respectively. The port diameters at the forward end at the onset of oscillations are about 36~37 mm. Oscillations, did not, however, occur in No. 26, in which the shape of the grain was close to that of Nos. 11, 24, and 25 at the time T_g. Furthermore, oscillation did not occur in No. 27, contrary to the authors' expectation. These results suggest that oscillation does not occur under the initial condition when the growth rate is close to or larger than the decay rate, although it generally occurs when the growth rate overcomes the decay rate. Therefore, it follows that initiation of oscillation requires an induction time of less than 0.5 sec. On the other hand, oscillation, once it occurs, continues until the grain burns out, even though a remarkable pressure change is provided as shown in the pressure-time histories of S-310 or No. 2 in Fig. 3a. These interesting phenomena must be solved by further experimentation. As the grain configurations in Nos. 24-27 do not always precisely simulate the instantaneous burning configuration of No. 11, these phenomena must be examined in more detail. This can be done by means of an experiment on extinction and reignition of a test motor.

Stable-Unstable Criterion

The existence of oscillation in a motor is generally estimated from a sign of the sum of the growth rate due to combustion (α_b) and a decay rate which consists of the contributions associated with the nozzle (α_n); particles in the combustion gas (α_p) and the chamber wall (α_c); and so on. R. L. Coates and M. D. Horton proposed a stable-unstable criterion related to the oscillation using the following expressions about α_b, α_n, α_p, and α_c [1,4]

$$\alpha_b = kf(L/2) \quad (\bar{P}_A/\bar{P}_V)^2 (A/V) \tag{1}$$

$$\bar{P}_A{}^2 = (1/A)\int_A P^2 \mathrm{d}A$$

$$\bar{P}_V{}^2 = (1/V)\int_V p^2 \mathrm{d}V$$

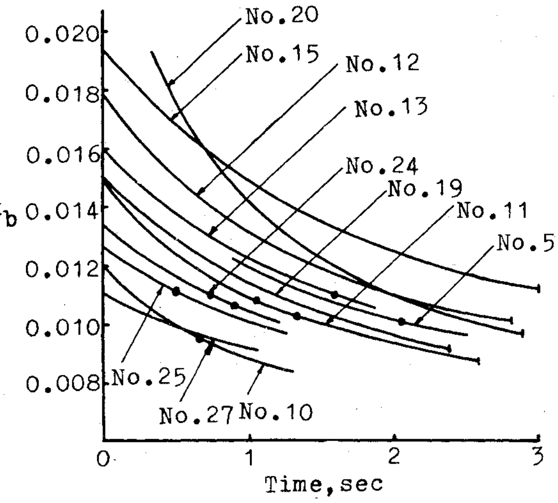

Fig. 4 Some k_b changes with burn time.

$$k = \alpha_{bT}/f$$

$$\alpha_n \simeq -2fJ \tag{2}$$

$$\alpha_p \simeq -0.34\ Xf \tag{3}$$

$$\alpha_c \simeq 0 \quad \text{(in an internal burning grain)} \tag{4}$$

where f = frequency, L = chamber length, A = burning area, V = chamber volume, p = amplitude of oscillating pressure, α_{bT} = growth constant obtained from a T-burner test with end-burning propellant, and X = weight fraction of solids in the exhaust. The relation $\alpha_b + \alpha_n + \alpha_p + \alpha_c < 0$ holds in the stable condition, so that Eqs. (1-4), yield the following inequality

$$k < 2(2J + 0.34X)(\bar{P}_V/\bar{P}_A)^2 (V/AL) \tag{5}$$

This inequality shows that the initiation of oscillation is difficult as J and V/AL increase, the latter being inversely proportional to L/D in a cylindrically perforated grain. This prediction agrees with the results obtained in the authors' experiments. Denoting the right-hand side of Eq. (5) by k_b, the equality $k = k_b$ holds true at the instant oscillation begins. The k_b time histories of several motors used in the authors' investigations are shown in Fig. 4. The dots on the lines indicate the initiation time as was obtained experimentally. This figure shows that every oscillation occurred at a time when k_b was in the range 0.009~0.012. Assuming the k of this propellant to be 0.011, T_g can be predicted and confirmed with the experimental results as shown in Table 6. Among these results, Nos. 19-22, 26, and 27 do not show oscillation experimentally, although they are predicted to initiate oscillation. These disagreements may be explained, however, from the port divergence effect and the insufficient induction time. Hence, from an engineering standpoint, most of the predicted T_g's agree with the experimental results. Therefore, the previously mentioned stable-unstable criterion associated with a few results obtained in the authors' investigation would be more useful in motor designing.

Suppression Devices

Single Orifice Baffle

Although oscillation occurs at 1.3 sec after ignition in No. 2 (as shown in Table 1), it does not occur in Nos. 28 and 29 (in Table 7), which have single orifice baffles made of 5-mm thickness FRP (manufactured from glass and phenolic resin).

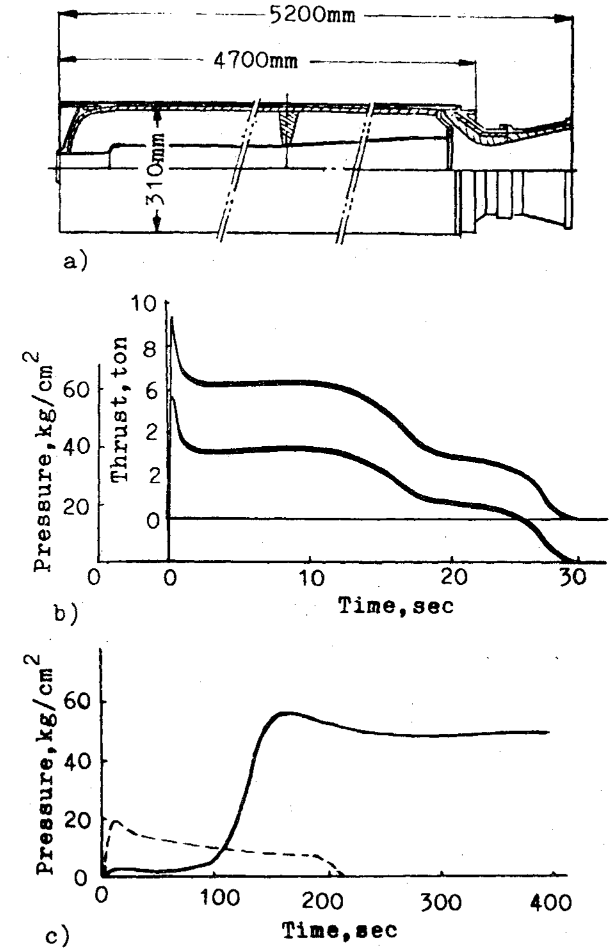

Fig. 5 a) Sounding rocket S-310 with a baffle. b) Pressure and thrust-time histories. c) Relation between pressure in an igniter and in a motor.

These two have inner diameters of 20 mm and 30 mm, respectively. The port diameters at the vicinity of the baffles in these motors are calculated as 41 mm at 1.3 sec after ignition. These 20 and 30 mm i.d. baffles will narrow the gas flow port to 24% and 54%, respectively, at 1.3 sec. In the case of No. 30, where the baffle inner diameter is 45 mm, oscillation occurs as well as in No. 2 at 1.3 sec after ignition, when the baffle is not yet exposed to the burning surface. However, oscillation disappears at 2.5 sec, when the calculated port diameter of the grain at the vicinity of the baffle is 60 mm and the baffle narrows the gas flow port to 56%. These results suggest that oscillation can be suppressed if a baffle located at the midpoint of the motor narrows the gas flow port to about 50%. However, this figure will depend upon various parameters such as grain configuration and propellant composition.[5,6]

Grooves

Narrow grooves of 4 mm width are provided on the circumference of the grain port as shown in Nos. 32-34. The combustion gases ejected from the grooves may disturb the main flow and suppress oscillation. However, oscillation occurs in every motor so that grooves are not useful to suppress oscillation; but T_g tends to be increased in a motor of which grooves are close to both ends of the grain.

Applications to S-310 Rockets

Some investigators have suggested that the number of oscillations decreases as the amount of aluminum agglomeration on the propellant burning surface decreases.[7,8] Therefore, a propellant with less agglomeration was applied to the sounding rocket S-310 in the second firing test, which consisted of 17% polybutadiene, 64% ammonium perchlorate, 14% aluminum, and 4% additives. In this test, however, oscillation occurred in much the same manner as in the first firing, indicating that the longitudinal pressure oscillation does not depend upon an aluminum agglomeration on the burning surface.

The third S-310 test motor was provided with a baffle at the midpoint of the grain, since this proved to be very effective in simulation motor No. 31. The results of the test were that the first mode oscillation did not occur, but the second mode longitudinal oscillation with an amplitude of 0.2 ~ 0.3 kg/cm^2 and with frequency of about 240 Hz began at 0.5 sec after ignition, as shown in Fig. 5. In this case, the thrust oscillation amplitude was very small, due not only to the decreased pressure amplitude, but also probably because the pressure waves at both ends of the chamber always had the same sign, that of the second mode longitudinal oscillation which, therefore, resulted in the canceling of thrust argumentation. The cross sections of the forward- and aft-end propellant grain and the shape of the igniter are similar to those shown in Fig. 1a. The only difference is that the amount of the igniter charge increased in this case. Figure 5c shows the relation between the pressure in the igniter (dotted line) and in the rocket motor (solid line).

Conclusions

These experimental results lead to the following conclusions concerning the relation between first-mode longitudinal oscillations and grain configurations or suppression devices. 1) Small steps or edges in a grain have a tendency to cause longitudinal pressure oscillation. Port configurations widening stepwise above a certain angle have an especially great influence. 2) The time required for initiation of oscillation increases with increasing nozzle throat diameter or decreasing grain slenderness. 3) The initiation of oscillation requires an induction time of less than 0.5 sec. 4) Oscillation, once occurring, continues until the propellant grain burns out. 5) The baffle is a very effective device for suppressing a longitudinal pressure oscillation, but it will make a higher mode oscillation under some conditions. The groove is not as effective. 6) The stable-unstable criterion for the longitudinal pressure oscillation proposed by R. L. Coates and M. D. Horton is very useful when the results mentioned in 1) and 3) are added.

References

[1] Hart, R. W. and McClure, R. T., "Theory of Acoustic Instability in Solid Propellant Rocket Combustion," 10th Symposium (International) on Combustion, Aug. 1964, pp. 1047-1065.

[2] Coates, R. L. and Horton, M. D., "Design Considerations for Combustion Stability," *Journal of Spacecraft and Rockets*, Vol. 6, March 1969, pp. 296-302.

[3] Culick, F. E. C. and Levine, J. N., "Comparison of Approximate and Numerical Analyses of Nonlinear Combustion Instability," AIAA Paper 74-201, Washington, D.C., Jan.-Feb. 1974.

[4] Slates, R. O., Buffum, F. G. and Dehority, G. L., "Acoustic Attenuation in Resonant Model-Rocket Motors," ICRPG/AIAA, Second Solid Propulsion Conference, Anaheim, Calif., June 1967.

[5] Oberg, C. L., Haymes, W. G. and Wong, T. L., "Solid Propellant Combustion Instability Suppression Devices," AIAA Paper 71-1051, New Orleans, La., 1972.

[6] Colucci, S. E., "Mechanical Suppression Devices to Stabilize Solid Rocket Motors," AIAA/SAE 9th Propulsion Conference, Las Vegas, Nevada, Nov. 1973.

[7] Watermeier, L. A., Angst, W. P. and Pfaff, S. P., "An Experimental Study of the Aluminum Additive Role in Unstable Combustion of Solid Rocket Propellants," *9th Symposium (International) on Combustion*, Aug.-Sept. 1962, pp. 316-327.

[8] Tough, L. H., "Motor Development for the Black Blant VB," AIAA Sounding Rocket Specialist Conference, Feb.-Mar. 1967, pp. 280-286.

[9] Karnesky, A. L. and Colucci, S. E., "Recent Occurrences of Combustion Instability in Solid Rocket Motors – An Overview," *Journal of Spacecraft and Rockets*, Vol. 12, Jan. 1975, pp. 33-38.